Science Arts & Métiers (SAM)

is an open access repository that collects the work of Arts et Métiers ParisTech researchers and makes it freely available over the web where possible.

To cite this version :

Estimated stress and friction distributions on tool rake face in the medium density fiberboard cutting process

Jean-Philippe Costes

Cyrille Decès-Petit

Yusuf Altintas

Pak Ko

Abstract

This paper presents a model of load distribution on the cutting edge of a tool during machining medium density fiberboard (MDF). A series of cutting tests was carried out with tools having designated rake face contact lengths. Utilizing the experimental data and a mechanics approach developed earlier by the third author, a model to estimate the distribution of stresses and friction on the rake face was developed. The model provides an essential step in the design and development of cutting edge geometry to prevent early edge failure and to control and reduce thermal/mechanical loading of the tool wedge.

The mechanics of metal cutting has been studied extensively. As a result, the design of cutting tools and the choice of machining parameters have been fairly successfully optimized. In the case of wood cutting, although there has been considerable research done, the knowledge that can be practically applied appears pale compared to the more mature research knowledge in metal cutting.

The major work in the mechanics of wood cutting began in the 1950s by Kivimaa (1950), Franz (1958), and McKenzie (1960). McKenzie introduced two numbers to describe three basic types of orthogonal cutting of green wood. One is the angle, which is either normal (90 degrees) or parallel (0 degrees), between the cutting edge of the tool and the cellular grain direction. The other is the angle between the direction of cutting and the grain direction. McKenzie and Franz further described the various types of chips that would be expected under different tool geometry and cutting conditions. These researchers have also performed a great number of orthogonal cutting tests to study the relationship of tool forces with rake angle and chip thickness for several green and dry wood species. In medium density fiberboard (MDF) machining, Stewart (1989) found good correlation between cutting forces and edge recession on C2 tungsten carbide tools with different rake angles. His results indicate that moderate rake angles between 10 and 30 degrees are optimum for C2 tungsten carbide tools. Stewart also published the results of a study involving 20 different tool materials, coatings, and surface treatments (Stewart 1991). He found that diamond (PCD) and C2 carbide have the lowest cutting forces and tool wear. More recently, Suzuki et al. (1997), in a low-speed orthogonal cutting study, presented the results of the effects of clearance angle and depth of cut on the machinability of MDF. From a linear cutting experiment of MDF using a modified milling machine, McKenzie et al. (1999) developed a set of equations relating the cutting forces with the feed rate and the layer density of MDF.

A finite element technique has been attempted in wood cutting studies (Holmberg 1998). However, because wood is an anisotropic material, there is a considerable challenge in modeling the influence of grain direction and the changes in material properties along the
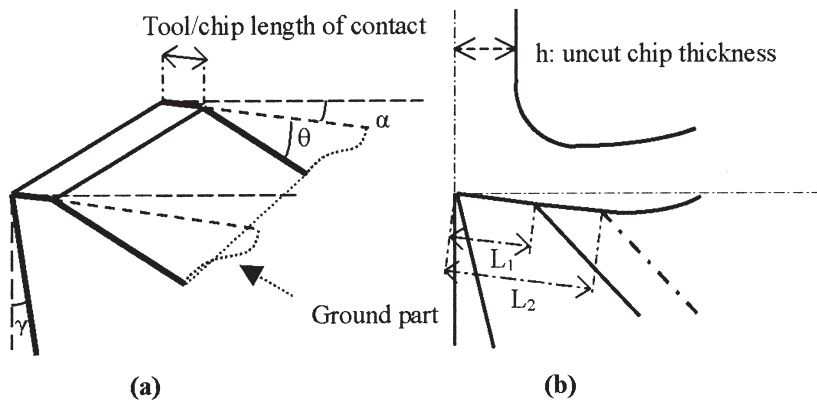
Forest Prod. J. 53(11/12):

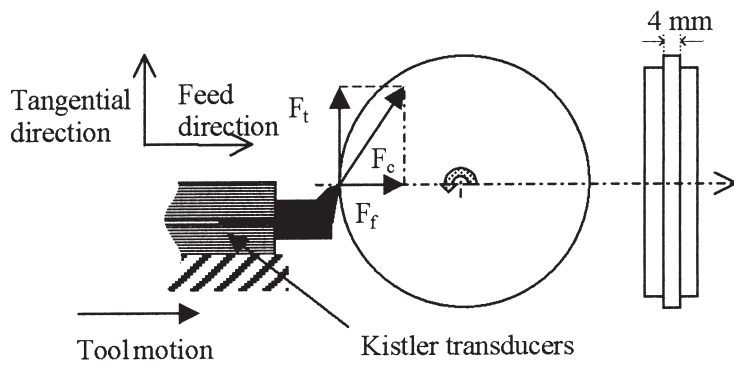Figure 1. — Preliminary tool grinding process.

Figure 2. — Experimental set-up in plunge turning of MDF. The tangential (F_t) and feed (F_f) forces are measured with a Kistler Dynamometer.

Table 1. — Experimented feed rates for tool number i.

Tool no.	Tool-chip contact length	Feed rates			
i	L_i	$h^i_{0.25} = 0.25 \cdot L_i$	$h^i_{0.5} = 0.5 \cdot L_i$	$h^i_{0.75} = 0.75 \cdot L_i$	$h^i_1 = L_i$
		$h^i_{1.25} = 1.25 \cdot L_i$	$h^i_{1.5} = 1.5 \cdot L_i$	$h^i_{1.75} = 1.75 \cdot L_i$	$h^i_2 = 2 \cdot L_i$

cutting direction. Although, it is possible to predict the direction of failure in solid wood, it is difficult to predict the cutting forces, due to the unpredictable variations of material properties. In Holmberg's finite element model, he superimposed several layers of isotropic material with incremental mechanical properties to simulate the orthotropic structure of wood. However, the simulated cutting speed in the model was much lower than that in a realistic wood cutting process. MDF, which is closer to an isotropic material, can be expected to give more consistent results and is therefore more suitable for studying the fundamentals of wood cutting.

MDF can be assumed to have uniform material property on the surface, al-though its hardness and density decrease rapidly toward the core. Dippon et al. (2000) presented an orthogonal cutting test strategy to extract average friction and normal forces acting on the tool. They developed a set of constants in terms of tool rake angle, layer depth (micro-hardness), and feed rate for cutting MDF. These orthogonal cutting constants were transformed to an oblique plane of cut, allowing accurate prediction of cutting forces for routers having an arbitrary geometry (Engin et al. 2000). In their model, the friction and normal load on the cutting tool were considered as point loads. In the present study, the distribution of these forces on the rake face is investigated, which

could provide essential information for the design of tool edge geometry.

In this present work, tools with restricted tool-chip contact lengths were studied in order to map the friction and normal load distribution between the rake face and chip in machining MDF. This paper presents the results of a series of orthogonal cutting tests using tools with different contact lengths and empirical equations for the prediction of friction and load distributions.

Experimental set-up

Cutting tests were performed on a **CNC** lathe using a set of carbide tools with a 10-degree clearance angle (γ) and a 10-degree rake angle (α) on MDF discs 400 mm in diameter. The carbide tools were ground on the rake face with a 30-degree secondary rake angle (θ) and each with a different contact length L_i (**Fig. 1**). The tool-chip contact is adjusted to the desired length L_i by changing the grinding location along the rake face. The purpose of restricting the rake face contact length is to control the contact of the cut chip with the rake face. Sixteen tools were ground to varying contact lengths from 0.05 mm to 1.5 mm.

The MDF discs were initially machined with a peripheral recess 5 mm deep on both sides, leaving a 4-mm-wide rib in the middle (**Fig. 2**). For the cutting tests, the MDF disc was fixed to a metal plate, which was attached to the spindle of the lathe. Orthogonal cutting was carried out on the periphery edge of the rib with the tool moving in the radial direction toward the center of the disc (**Fig. 2**). Since the width of the tool cutting edge is larger than 4 mm, the process is truly orthogonal without any side contact between the sides of the tool cutting edge and the MDF. Furthermore, for each disc, the same layers of MDF material were machined. The cutting speed was set to a constant value of 4 m/sec. For each tool, eight tests were performed at different uncut chip thickness h by adjusting the feed rate (**Table 1**).

A three-components Kistler force dynamometer (9257 B) was set up to measure the feed force (parallel to the direction of tool motion or feed) F_f, and the tangential force (normal or perpendicular to the direction of tool motion) F_t. The data were collected at a rate of 2,000 samples per second and then filtered
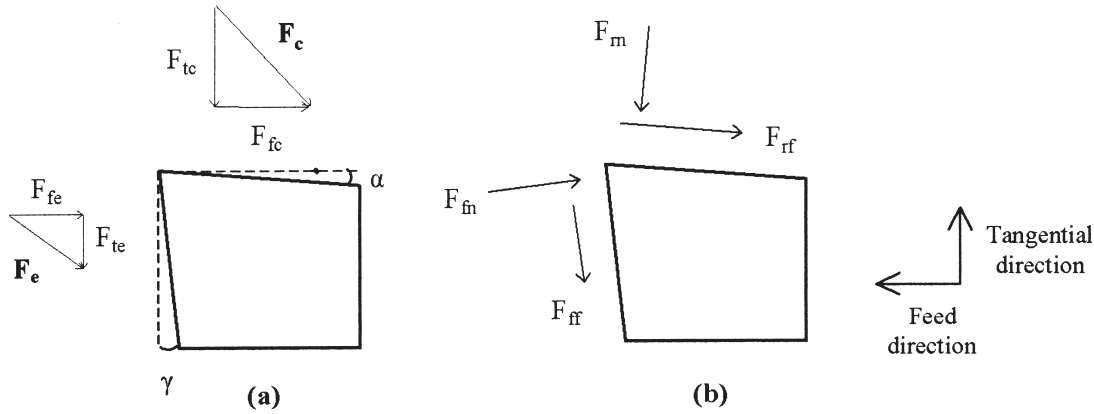
Figure 3. — Free-body force diagrams of the tool in orthogonal cutting.

with a low-pass filter set at 30 Hz cut-off frequency.

Cutting force model

In metal cutting, it is possible to express the forces on the rake face as a function of the shear stress, the average tool-chip contact friction, and shear angle (Altintas 2000). In the case of wood cutting, the process involves a different chip fracture mechanism and a heterogeneous material, therefore the equations derived for metal cutting based on shear failure are not applicable. Earlier, a mechanistic model was developed that de-couples the forces into rake and flank components (Dippon et al. 2000). This model is adopted in the present article for the development of the load distribution equations.

The process considered here is an orthogonal cutting operation where the cutting edge is perpendicular to the cutting velocity, hence the process is two-dimensional with zero forces in the radial direction. In the orthogonal cutting process, two fundamental cutting forces, the tangential force F_t and the feed force F_f (**Figs. 2** and **3**) are considered. Each of these two cutting forces is resolved into two parts, the edge force F_e, which results from the contact between the flank face and the finished MDF surface, and the chip force F_c, which acts on the chip-tool rake face contact zone.

The edge force F_e is further resolved into the two parts: tangential edge force F_{te}, which is parallel to the cutting speed, and the feed edge force F_{fe}, which is perpendicular to the cutting speed. Similarly, the chip force F_c is also resolved into the tangential chip force F_{tc} and feed chip force F_{fc} components (**Fig. 3a**). Considering a sharp edge, we

assume in this study that F_e is applied at the edge as a line force, while F_c is applied on the rake face. If the chip force is assumed to be proportional to the uncut chip area, and the edge force is related to the width of cut only, equations for the tangential and feed forces can be constructed. Thus:

$$F_t = F_{tc} + F_{te} = K_{tc}bh + K_{te}b \quad [1]$$

$$F_f = F_{fc} + F_{fe} = K_{fc}bh + K_{fe}b$$

where:

$$h = \text{uncut chip thickness}$$
$$b = \text{width of cut}$$
$$K_{tc}, K_{fc} \text{ and } K_{te}, K_{fe} = \text{chip and edge cutting coefficients, respectively}$$

For zero uncut chip thickness, $h = 0$, we assume that the chip forces F_{tc} and $F_{fc} =$ zero. Thus:

$$F_{te} = F_t \text{ and } F_{fe} = F_f \text{ for } (h = 0) \quad [2]$$

Experimentally, the tangential and feed forces are obtained from cutting tests with incremental feed rates. Since the edge force components F_{te} and F_{fe} are independent of the chip thickness h, and can be obtained from F_t and F_f extrapolated to $h = 0$, the chip force components F_{tc} and F_{fc} can be obtained by subtracting the edge forces from the measured forces F_t and F_f giving:

$$F_{tc} = F_t - F_{te} \quad [3]$$

$$F_{fc} = F_f - F_{fe}$$

From **Figure 3b**, the normal and friction force components, respectively F_{rn}, F_{fn}, on the rake face can be expressed as:

$$F_{rf} = F_{fc} \cos \alpha + F_{tc} \sin \alpha,$$

$$[4]$$

$$F_{rn} = F_{tc} \cos \alpha - F_{fc} \sin \alpha$$

We assume that the friction on the rake face satisfies a Coulomb friction model; therefore, the average friction coefficient on the rake face μ_r can be evaluated using:
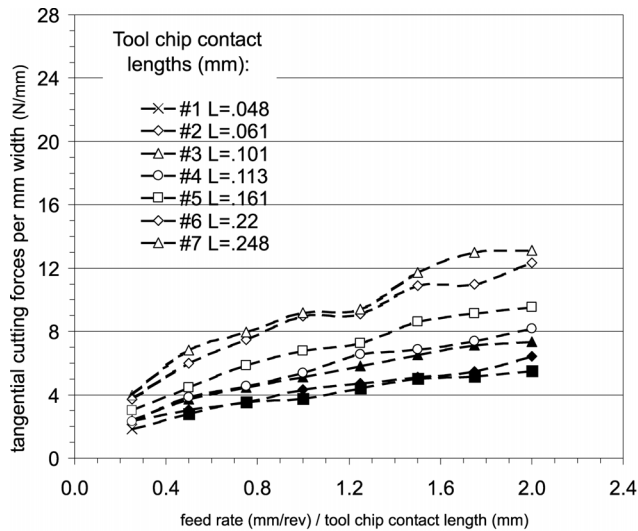
$$\mu_r = \frac{F_{rf}}{F_{rn}} = \frac{F_{fc} \cos \alpha + F_{tc} \sin \alpha}{F_{tc} \cos \alpha - F_{fc} \sin \alpha} \quad [5]$$

Thus, for a given uncut chip thickness h, Equation [5] gives the average friction coefficient on the rake face.
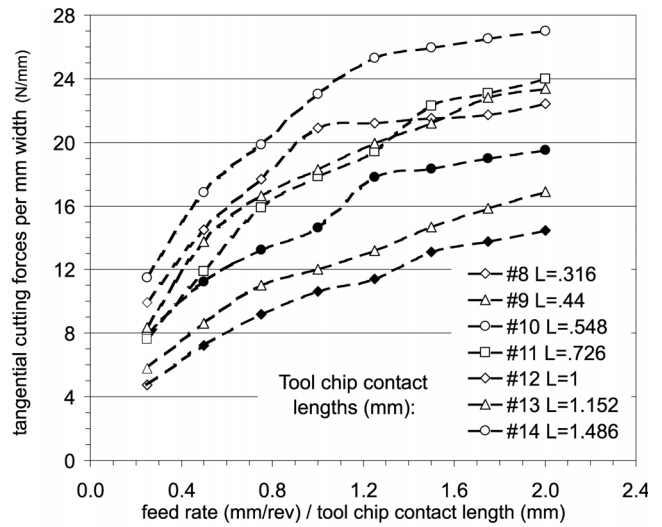
Experimental results

The 16 tools with different tool-chip contact lengths were tested for 8 increments in chip thickness (feed rate) covering a range up to 2 times the tool-chip contact length. For each test, the feed and tangential components of the cutting forces were measured. In order that the force data from a number of tests can be displayed on the same figure, the chip thickness (or feed rate) parameter was normalized with the tool-chip contact length of the respective test.

The 16 sets of data were divided into two groups and plotted in **Figures 4a** and **4b**, which show the measured cutting forces per unit chip width in the tangential direction vs. the normalized chip thickness. The tangential force appears to increase fairly linearly, with the exception of the ones having tool-chip contact length longer than 0.5 mm, with increasing normalized feed rate. The curves of the 16 tests also appear to be positioned fairly regularly in an ascending order with the shortest tool-chip-contact-length curve occupying the lowest position (**Fig. 4a**) and the longest tool-chip-contact-length curve occupying the uppermost position (**Fig. 4b**).
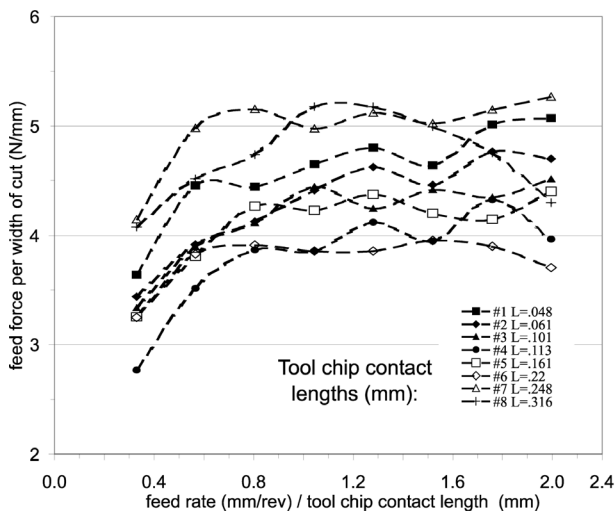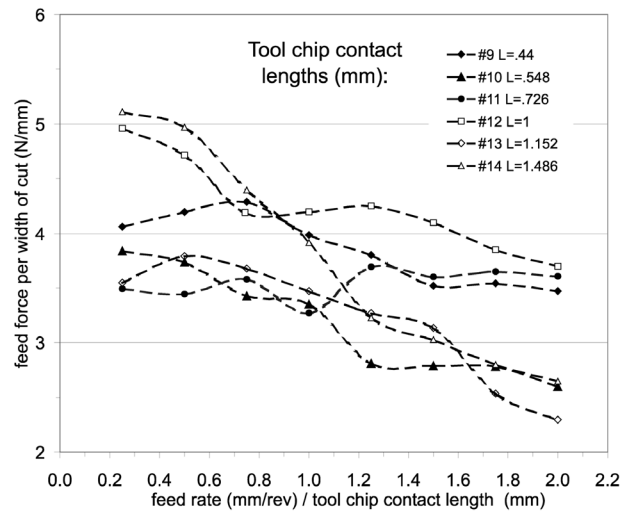
Figure 4. — Tangential forces results. For each tool, the measured forces are shown in respect to the ratio feed rate/tool chip contact length. Tangential forces are normalized in respect to cutting width. Figure 4a shows the results for tools 1 to 7. Figure 4b shows the results for tools 8 to 14.
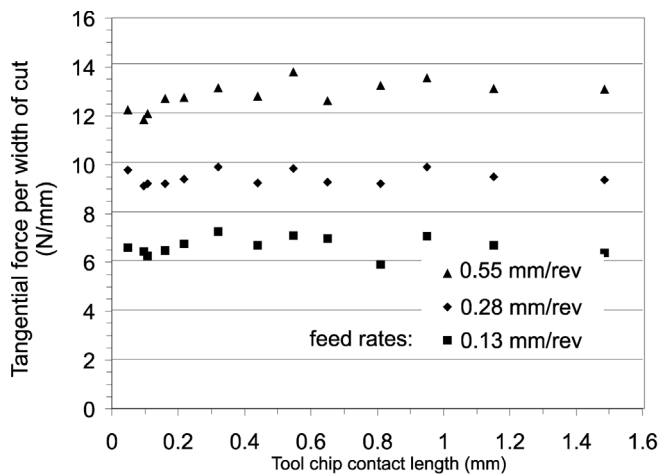

Figure 5. — Feed forces results. For each tool, the measured forces are shown in respect to the ratio feed rate/tool chip contact length. Feed forces are normalized in respect to cutting width. Figure 5a shows the results for tools 1 to 8. Figure 5b shows the results for tools 9 to 14.

The curves with tool-chip contact length longer than 0.5 mm appear to increase linearly at first until the normalized feed rate reaches around one, that is, the actual feed rate equals the tool-chip contact length. Then the curves change abruptly, each to a new linear curve with a much lower rate of increase.

The corresponding feed forces (per unit chip width) were also plotted against the normalized feed rates and are displayed in two groups (**Figs. 5a** and **5b**). Contrary to the tangential forces shown in **Figure 4**, the positions of the feed-force curves with different tool-chip contact lengths appear to be at random. For tools with longer tool-chip contact length, a hint of decreasing feed force with increasing normalized feed rate exists. However, the pattern is highly irregular and does not follow any order of the tool-chip contact length (**Fig. 5b**). On the other hand, for tools with shorter tool-chip contact lengths, the feed force appears at first to increase with the normalized feed rate until this ratio reaches about one. Then the feed force remains more or less constant with further increase in the normalized feed rate (**Fig. 5a**). The overall variation of the feed forces appears to cover a very narrow range from 2.5 N/mm to 5 N/mm. Small variations in other test pa-
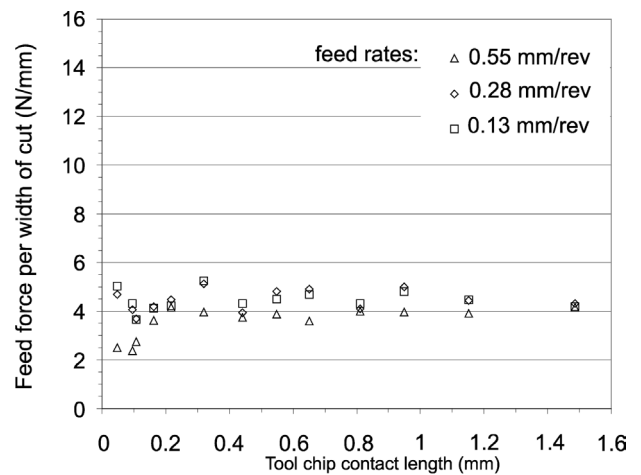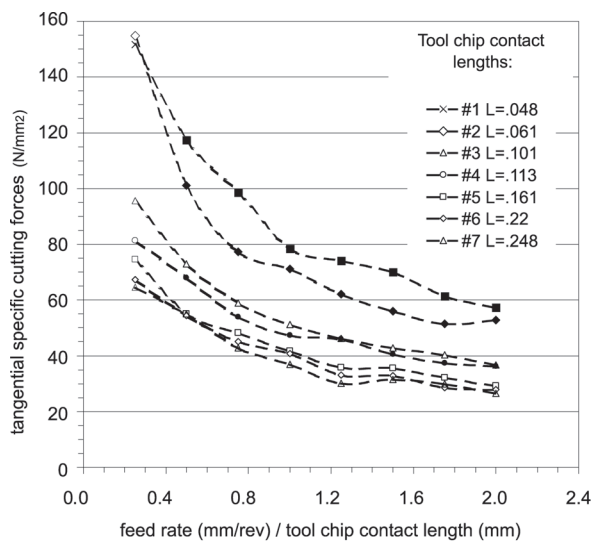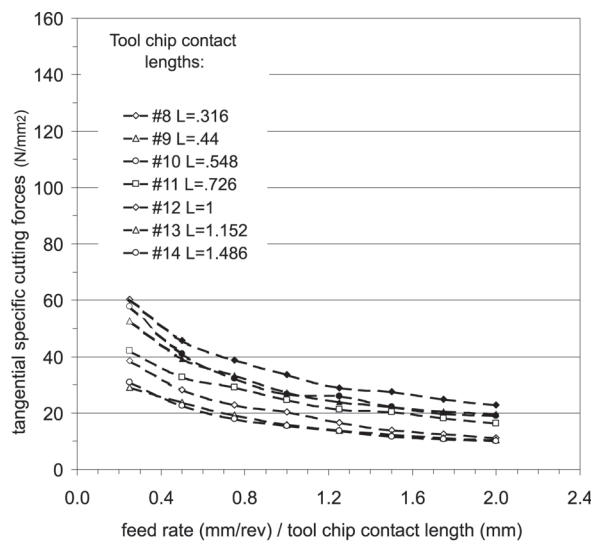
Figure 6. — Tangential (a) and feed (b) forces results for three feed rates and increasing tool-chip contact lengths.

Figure 7. — Tangential specific forces results. For each tool, the specific forces are shown in respect to the ratio feed rate/tool-chip contact length. Figure 7a shows the results for tools 1 to 7. Figure 7b shows the results for tools 8 to 14.

rameters could have resulted in the apparent changes in the feed forces.

To clarify the results observed in **Figures 4** and **5**, a new set of tests was carried out for the tangential and feed forces versus tool-chip contact lengths with the feed rate kept constant in each test. **Figures 6a** and **6b** show respectively the tangential force and the feed force vs. tool-chip contact length for three feed rates. The results clearly show that the tool-chip contact length has no effect on the tangential force. Rather, the tangential force increases with increasing feed rate. The feed forces shown in

Figure 6b appear to be independent of the tool-chip contact length and are within the range of 4 N/mm to 5 N/mm for the three feed rates tested. At the feed rate of 0.55 mm/rev, it appears that both the tangential force and the feed force increased with increasing tool-chip contact length for the very short lengths up to about 0.3 mm. It is postulated that for tools with a very short tool-chip contact length on the rake face, the chip formation and flow may be different than the general chip formation process involving shear and deformation.

The tangential and feed forces (per unit chip width) shown in **Figures 4** and **5** were further normalized by dividing each with the respective tool-chip contact length to obtain the corresponding specific cutting forces (per unit tool-chip contact area on the rake face). The specific tangential forces versus the normalized feed rates are shown in **Figures 7a** and **7b** for the two groups of tools having the shorter and longer tool-chip contact lengths. The corresponding specific feed forces are shown in **Figures 8a** and **8b**. Interestingly, the specific tangential forces now decrease with increasing normalized feed rates and the effect
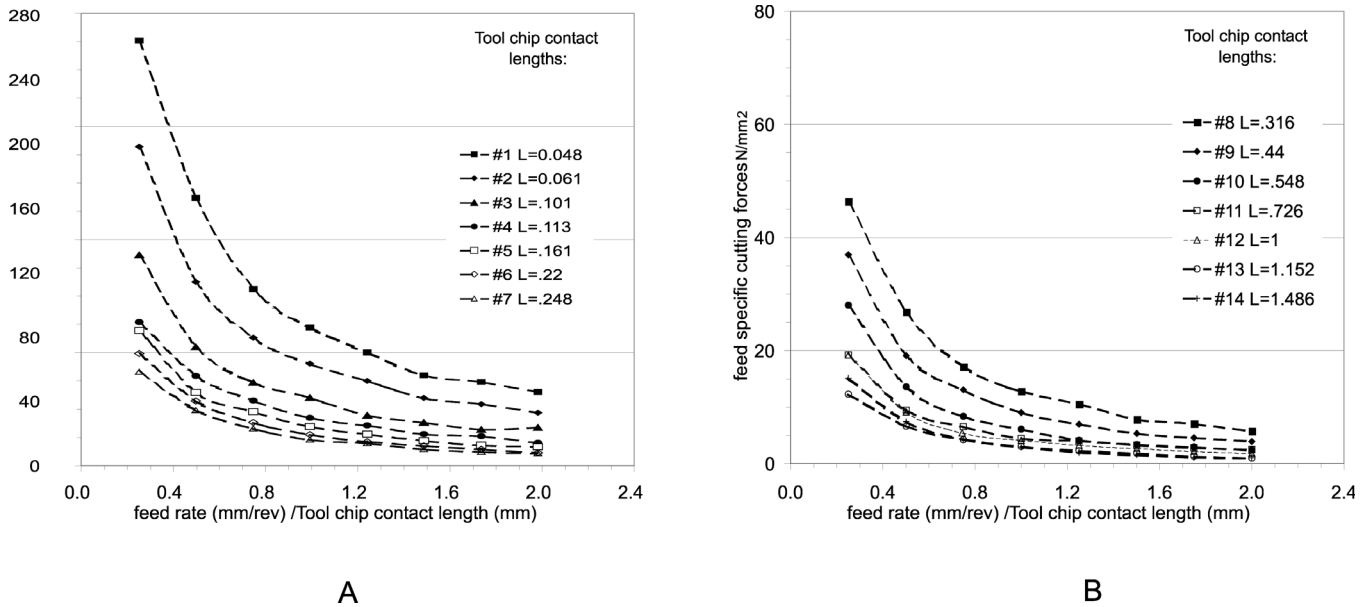
A

B

Figure 8. — Feed specific forces results. For each tool, the specific forces are shown in respect to the ratio feed rate/tool-chip contact length. Figure 8a shows the results for tools 1 to 7. Figure 8b shows the results for tools 8 to 14.
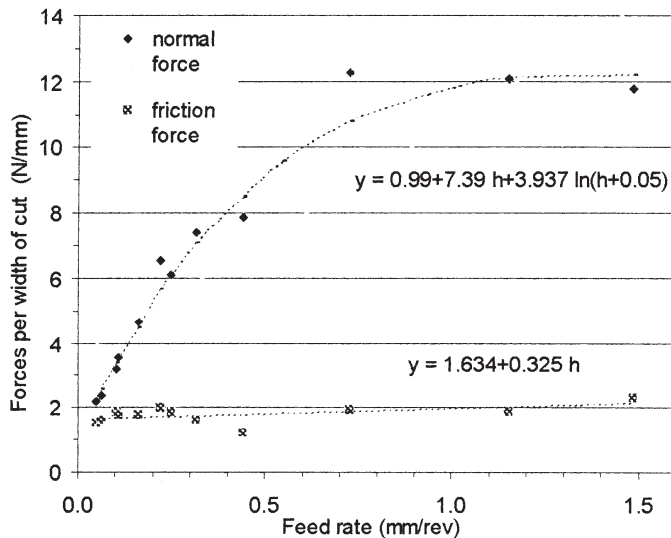

Figure 9. — Friction and normal forces F_{rn} and F_{rf}. F_{rn} and F_{rf} are resulting from the projection of the chip force along the rake face in parallel and orthogonal direction. Only values where the feed rate is equal to the tool-chip contact length have been considered.

of tool-chip contact length is reversed with the force curves appearing in a descending order for increasing tool-chip contact lengths. Of particular interest is the specific feed forces. They were transformed from a highly irregular pattern to an orderly display of the effects of normalized feed rate and tool-chip contact length. The specific feed force generally decreases with increasing normalized feed rate and also decreases with increasing tool-chip contact length. In all cases, with both the specific tangential force and specific feed force, the effect of the normalized feed rate appears to be pronounced until it reaches about one, that is when the actual feed rate equals the tool-chip contact length. For normalized feed rates higher than one, the specific cutting forces tend towards constant. In other words, the ef-

fect of the normalized feed rate diminishes to zero.

Distribution of normal and friction forces

The measured cutting forces were extrapolated to obtain the feed and tangential forces at zero chip thickness (zero feed rate), which provide a set of constant values for the edge force components described in the previous section (Eq. [2]). As already described in the earlier section, the cutting forces acting on the rake face were obtained by removing the edge forces from the measured cutting forces (Eq. [3]). The feed and tangential components of the chip force on the rake face were further resolved to obtain the normal and friction forces on the rake face according to Equation [4]. The rake face forces measured in experiments where the normalized feed rate of one, that is, feed rate equals the tool-chip contact length, are plotted in **Figure 9** for each tool. One of the reasons for choosing these force values is that in the following calculations the chip load is assumed to distribute over the tool-chip contact area exactly, that is when the chip thickness (or feed rate) equals the tool-chip contact length.

F_{rn} and F_{rf} are normalized forces with respect to the width of cut ($b = 4$mm). It can be observed from **Figure 9** that the normal force-uncut chip thickness (equivalent to the feed rate) relationship
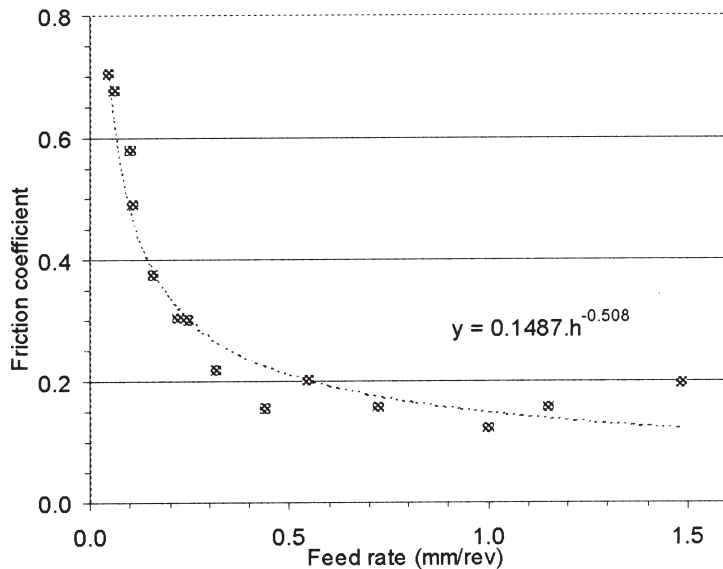
Figure 10. — Friction coefficient as a function of the feed rate; the friction coefficient is obtained by dividing F_{rf} by F_{rn}.
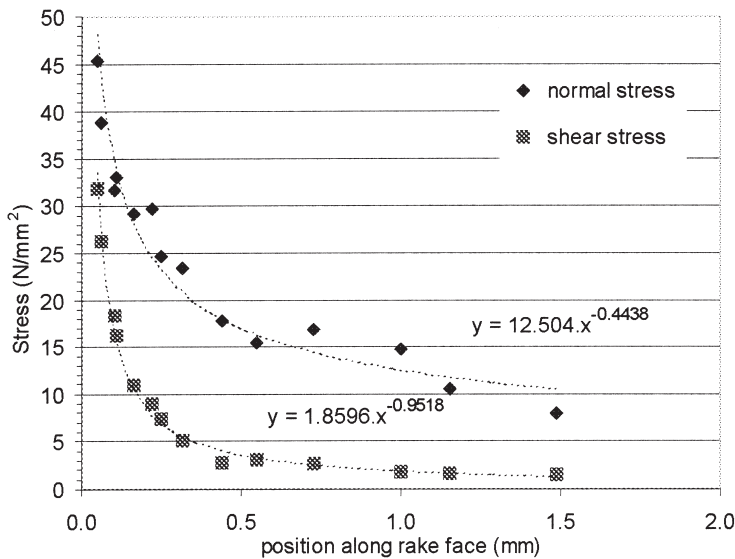
$$y = 0.1487.h^{-0.508}$$

Figure 11. — Normal and shear stress in respect to the position on rake face; values are obtained by dividing normal and friction forces by the tool-chip contact area.

$$y = 12.504.x^{-0.4438}$$

$$y = 1.8596.x^{-0.9518}$$

is logarithmic, whereas the friction force-uncut chip thickness is almost constant. The following empirical relationships were obtained by applying a least squares curve fit to the measured rake face forces:

$$F_{rn}(h) = \qquad\qquad [6]$$
$$0.99 + 7.39h + 3.937 \ln(h + 0.05)$$

$$Frf(h) = 1.634 + 0.325\,h$$

Using Equation [5] and the calculated normal and friction forces, the corresponding friction coefficients were ob-

tained and displayed in **Figure 10**. Again, applying a least square curve to fit the data, an equation is obtained for the average friction coefficient on the rake face μ_r in terms of the uncut chip thickness h.

$$\mu_r = 0.149.h^{-0.508} \qquad [7]$$

The results in **Figure 10** show that the coefficient of friction decreases rapidly with uncut chip thickness in the low chip thickness region, i.e., near the tool edge, and just as rapidly attains a near-constant value as the chip thickness is fur-

ther increased to about 0.4 mm and beyond. In metal cutting, the presence of a sticking region near the tool edge is now well known (Moore 1975), which contributes to a sharp increase in friction coefficient. In a separate friction experiment using the flat face of a piece of carbide tool material pressed and slid against MDF at a constant sliding speed, it was observed that initially the friction coefficient decreases rapidly with increasing applied normal load to around 0.1 (Styles 2002). The coefficient of friction became more or less constant and remained at about 0.1 as the applied normal force was increased to more than 100 N. Similar friction coefficient values around 0.12 have also been reported by others (Niedzielski et al. 2000).

Beyond the sticking region, the chip starts to slide over the rake face with a lower friction coefficient. Although friction in MDF machining is not well known, it seems that the chip cracks close to the cutting edge, and is compressed and trapped with limited motion close to the edge. It is then pushed out into the free zone on the rake face much like a dust without having a solid body energy. This may explain the low friction coefficient values, or the low friction forces.

Since the normal and friction forces shown in **Figure 9** have the units N/mm chip width, further dividing these forces by the tool-chip contact length h yields the average stresses, $\sigma_{average}$ and $\tau_{average}$, respectively, on the rake face. These stresses versus the uncut chip thickness (feed rate) are plotted in **Figure 11**. The curves in **Figure 11** show that the average stresses are very high for short tool-chip contact lengths and they decrease rapidly as the tool-chip contact length is increased to about 0.4 mm. At further increases from 0.4 mm to 1.5 mm, the stresses level off and attain very low values. For a first approach, it is therefore safe to assume that the tool-chip contact lengths could be substituted for the distances x from the tool edge to obtain the stress distribution along the tool rake face near the edge. Thus, the stress curves in **Figure 11** represent the average stress-distributions on the rake face. In later approaches, this stress model can be refined by reducing the influence of total contact lengths in the data. These estimated stress curves are represented by the following equations:

$$\sigma_{average} = 12.504 \cdot x^{-0.444} \qquad \textbf{[8]}$$
$$\tau_{average} = 1.86 \cdot x^{-0.952}$$

where:

   x = the contact position on the rake face from the cutting edge

$\sigma_{average}$, $\tau_{average}$ = the average normal and shear stresses acting on the rake face, respectively (MPa)

Dividing the expression for $\tau_{average}$ by the expression for $\sigma_{average}$ of Eq. [**8**] would yield the same logarithmic expression for the coefficient of friction shown in **Figure 10**.

The distribution of normal and friction stress on the tool along the chip contact zone indicates that the cutting edge is loaded most within 0.1mm, and almost diminishes after 0.25 mm when machining MDF. One can make a recommendation to tool manufacturers that the cutting wedge must be strongest within the first 0.25 mm of the rake, and the rake face can be ground with a secondary rake angle. The latter would lead to a reduction in friction force with the potential of reducing wear on the tool. The tool edge geometry can be optimally designed to resist the stresses on the tool by the pressure and friction distribution given above.

Conclusion

Unlike in metal cutting, where the process is dominated by plastic shear, machining MDF and wood is dominated by fracture and compression of MDF dust between the incoming material and the rake face of the tool.

This paper presents an approach to evaluate the friction and normal load distribution on the rake face of the tool for cutting MDF. The cutting forces are resolved into rake and flank components first. By limiting the rake face-chip contact lengths via restricted rake contact, the distributions of friction and normal stresses on the rake face are estimated. The results indicate that both friction and normal loading of the rake face decreases significantly within the first 0.25 mm of the contact. The information can be used to help estimate the stress

9485 P & P: This study presents a method to estimate the cutting forces distributions on the tool tip, which can be used to improve the tool geometry design, and provide a better understanding of the hard coating failure around the tool tip.

distribution on the tool face and hence better and optimal tool design. The results also point to the importance of hard coatings for wear protection applied to within the first 0.25 mm on the rake face, which can be then ground with a secondary rake angle to further minimize the friction between the restricted rake face contact and the chip. The design of the microbevel (Decès-Petit et al. 1999) on the tool edge can also be optimized using the information. Finally, heat generated by the chip can be also estimated by the stress distributions on the rake face.

Notations

  h = uncut chip thickness (mm)

  d = width of cut (mm)

F_t, F_f = tangential force, feed force (N)

F_c, F_e = chip force, edge force (N)

F_{tc}, F_{fc} = tangential and feed component of the chip force (N)

F_{te}, F_{fe} = tangential and feed component of the edge force (N)

F_{rn}, F_{rf} = normal and friction forces applied on the rake face (N)

K_{te}, K_{fe} = edge cutting force coefficients (in tangential and feed direction) (N/mm)

K_{tc}, K_{fc} = chip cutting force coefficients (in tangential and feed direction) (N/mm^2)

  μ_r = average friction coefficient of tool-chip contact on the rake face

  i = tool number

  L_i = rake face length of the tool i (mm)

Literature cited

Altintas, Y. 2000. Manufacturing Automation: Metal Cutting Mechanics, Machine Tool Vibrations, and CNC Design. Cambridge Univ. Press, New York. ISBN 0521650291.

Decès-Petit, C., P. Ko, and B. Cvitkovic. 1999. Influence of back microbevel on orthogonal wood cutting. *In*: Proc. 14th Inter. Wood Machining Seminar. **where could a reader obtain this?** pp. 397-405.

Dippon, J., H. Ren, F. Ben Amara, and Y. Altintas. 2000. Orthogonal cutting mechanics of medium density fiberboards. Forest Prod. J. 50(7/8):25-30.

Engin, S., Y. Altintas, and F. Ben Amara. 2000. Mechanics of routing medium density fiberboard. Forest Prod. J. 50(9):65-69.

Franz, N.C. 1958. Analysis of the Wood Cutting Process. Engineering Research Inst., Univ. of Michigan Press, Ann Arbor, MI.

Holmberg, S. 1998. A numerical and experimental study of initial defibration of wood. Rept. TVSM 1010. Lund Univ., Lund Institute of Tech., Sweden. 203 pp.

Kivimaa, E. 1950. Cutting force in wood-working. PhD thesis. Finland State Inst. for Tech. Research, **insert city**, Finland.

McKenzie, W.M. 1960. Fundamental aspects of the wood cutting process. Forest Prod. J. 10(9):447-456.

_____, P. Ko, R. Cvitkovic, and T. Ringler. 1999. Towards a model predicting cutting forces and surface quality in routing layered boards. *In*: Proc. 14th Inter. Wood Machining Seminar. **where could a reader obtain this?**

Moore, D.F. 1975. Principles and Applications of Tribology. Pergamon Press Ltd., Oxford, UK. pp. 250-254.

Niedzielski, P., S. Miklaszewski, P. Beer, and A. Sokolowska. 2000. Tribological properties of NCD coated cemented carbides in contact with wood. Diamond and Related Materials (10):1-6.

Stewart, H.A. 1991. A comparison of tool materials, coatings, and treatments related to tool wear during wood machining. Forest Prod. J. 41(9):61-64.

_____. 1989. Analysis of tool forces and edge recession after cutting medium density fibreboard. *In*: Proc. 9th Inter. Wood Machining Seminar. pp. 320-341. **where could a reader obtain this?**

Styles, E. 2002. Sliding friction tests of carbide tools on MDF. Tech. Rept. The National Research Council of Canada, Innovation Centre, Vancouver, BC, Canada.

Suzuki, S., J. Kobayashi, T. Tochigi, and H. Fukui. 1997. Machinability of medium density fiberboard. I. The effects of clearance angle and depth of cut on the machinability in end surface cutting. Mokuzai Gakkaishi 43(9):731-737.